

Supplementary Material for:

‘Collective dynamics of microtubule-based 3D active fluids from single microtubules’

Teagan E. Bate, Edward J. Jarvis, Megan E. Varney, and Kun-Ta Wu

Supplementary Information:

Coarsening of Microtubule Bundles. Dynamics of active fluids slowed down gradually over time (**Fig. 1D**). This decay was hypothesized to be related to structural change of active gels. To verify this hypothesis, microtubules were imaged in active gels at 20°C for 14 hr. In the beginning, microtubules were distributed mostly homogeneously, but over time, microtubules formed bundles that grew thicker (**Fig. S1**). Thickness growth enhanced image contrast, which allowed characterization of bundle coarsening by measuring the standard deviation of pixel values. The standard deviation increased with time, reflecting the growth of bundle thickness (blue in **Fig. S1C**). To examine whether the bundle coarsening caused the activity decay, the velocity field of microtubule bundle movements and their mean speeds as a function of time were measured (**Fig. S1B&C**)^{1, 2}. The mean speeds decreased over time accompanied by bundle coarsening, which suggested that the coarsening of microtubule bundles slowed down their movements. The slower bundle movements led to slower active fluid flows. Fortunately, this activity decay was slow and did not impact measurement results if the observation window was short. For example, at 20°C, bundle movements slowed from ~3 to ~2 $\mu\text{m/s}$ in 8 hr (**Fig. S1C**) but the decay effect was negligible during $t = 1\text{--}2$ hr, the chosen observation window.

Characterization of Microtubule Depolymerization. To examine the temperature dependence of the stability of GMPCPP-stabilized microtubules, microtubule lengths were monitored in microtubule gliding samples for 50 min at 10–20°C. However, gliding microtubules were motile and did not stay within a microscope field during the measurement window; therefore the sample was deprived of ATP to immobilize microtubules. The stationary microtubules were seen to shrink in lengths at 10°C whereas at 20°C the length was better preserved (**Fig. S2A**), similar to results of previous studies using taxol-treated microtubules³. To measure microtubule lengths, a filament tracking algorithm was used to trace microtubules in each image (pink curves), revealing microtubule length l decreased with time t . To characterize the length decay, the time-averaged rate of the length shrinking k was measured by fitting l vs. t to a line function, followed by extracting the line slope (inset in **Fig. S2B**). The time-averaged rates were measured for 10–13 microtubules to determine mean shrinking rate \bar{k} . The microtubules shrank below 16°C, implying microtubule depolymerization (**Fig. S2B**). Therefore, to ensure that microtubule depolymerization did not affect the investigation of active fluid dynamics, this analysis involved only temperature data at $\geq 16^\circ\text{C}$.

Temperature-Induced Malfunction for Kinesin Clusters. In this work, sample temperatures were varied to explore collective dynamics of active fluids. Maintaining fluid activity required kinesin to bridge pairs of microtubules while stepping toward microtubule plus ends (**Fig. 1A**). The dynamics required functional kinesin and formation of kinesin clusters. To ensure that both requirements were met, performance of kinesin clusters was examined in the explored temperature range, by adapting Böhm *et al.*'s method⁴. K401 motor clusters were pre-incubated at 20–40°C for 1 hr. The pre-incubated motors were used to prepare active fluid samples, in which time-averaged mean speeds of developed flows were measured at 20°C, and the mean speed was plotted as a function of the pre-incubation temperature (red dots in **Fig. S3A**). Mean speeds remained almost invariant (~5 $\mu\text{m/s}$) for the pre-incubation temperatures between 20 and 36°C. Above ~36°C, mean speeds dropped to ~0 $\mu\text{m/s}$, accompanied by microtubules developing into short, stationary bundles (top image in **Fig. S3B**). This result was in contrast to the cases without pre-incubation, in which microtubules developed into the long, extending bundles (**Fig. 1C**). These two observations suggested that K401 clusters were incapable of bridging and sliding pairs of microtubules after incubation at $>36^\circ\text{C}$.

In this work, non-processive motor K365 was also used. To examine temperature impact on K365 motor clusters, the same experiments were repeated. The K365 clusters remained stable at 20–40°C (blue dots in **Fig. S3A**). The motor clusters were able to drive microtubules into active gels after pre-incubation at 38°C (bottom image in **Fig. S3B**), suggesting that K365 clusters were more heat resistant than K401 clusters. While the underlying mechanisms causing such a difference remained an open question, in this work with both types of motors, the data was fitted, analyzed and compared at $\lesssim 36^\circ\text{C}$, to avoid the intervention of malfunctioning motor clusters in the analysis results.

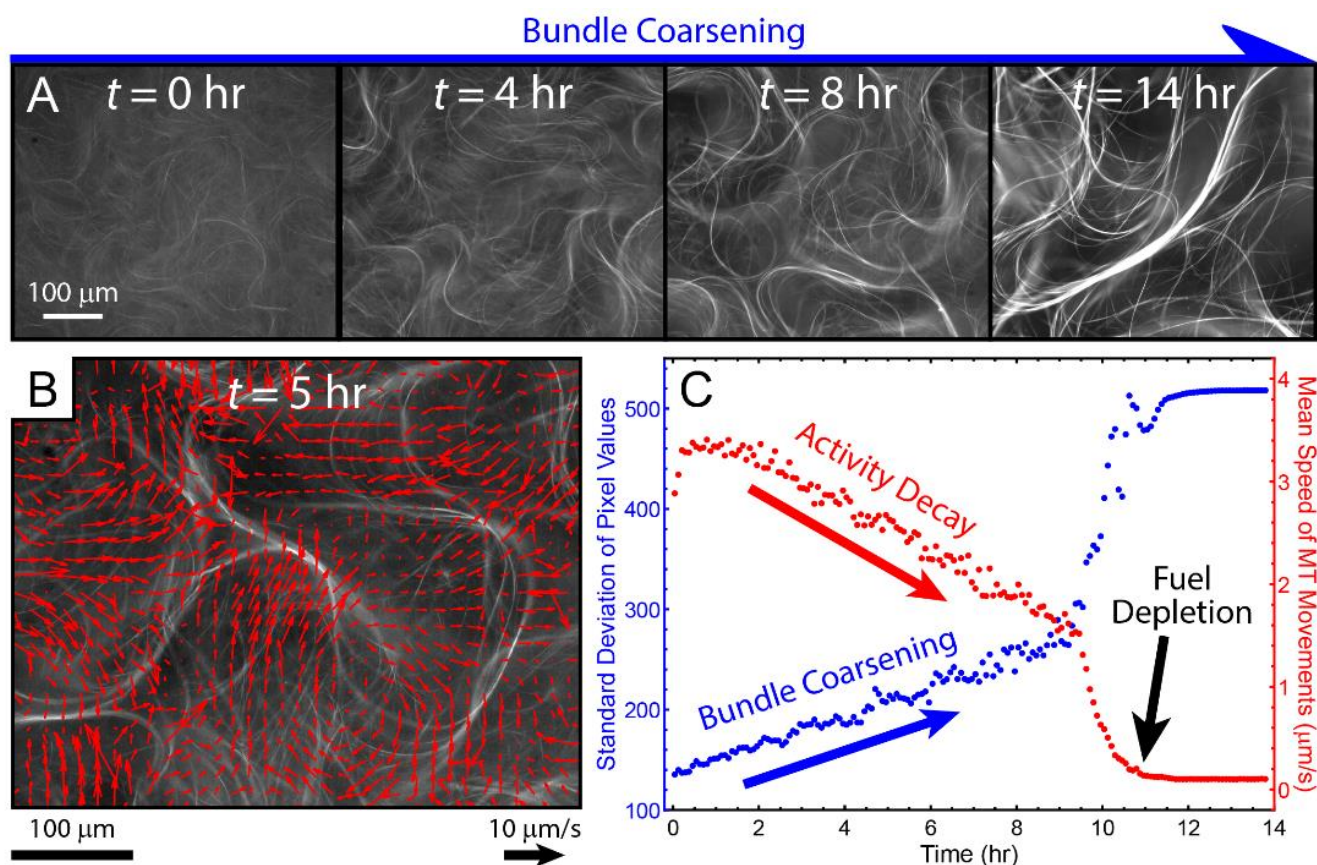


Fig. S1: Coarsening of Microtubule Bundles Causes Decays in Microtubule Activity. (A) Sequential images of microtubules at 20°C at $t = 0$ –14 hr. The microtubules formed bundles which coarsened over time. (B) Velocity fields of movements of microtubule bundles. The velocities were measured by tracking the motion of microtubule bundles with a particle-image-velocimetry algorithm (PIVlab version 2.02)^{1, 2}. (C) Standard deviation of pixel values in microtubule images compared with mean speed of microtubule movements. Bundle coarsening enhanced image contrast which increased standard deviation of the image's pixel values. The increase in the standard deviation was accompanied by the deceleration of microtubule movements, suggesting that bundle coarsening slowed down activity. Activity lasted for ~11 hr before fuel depletion.

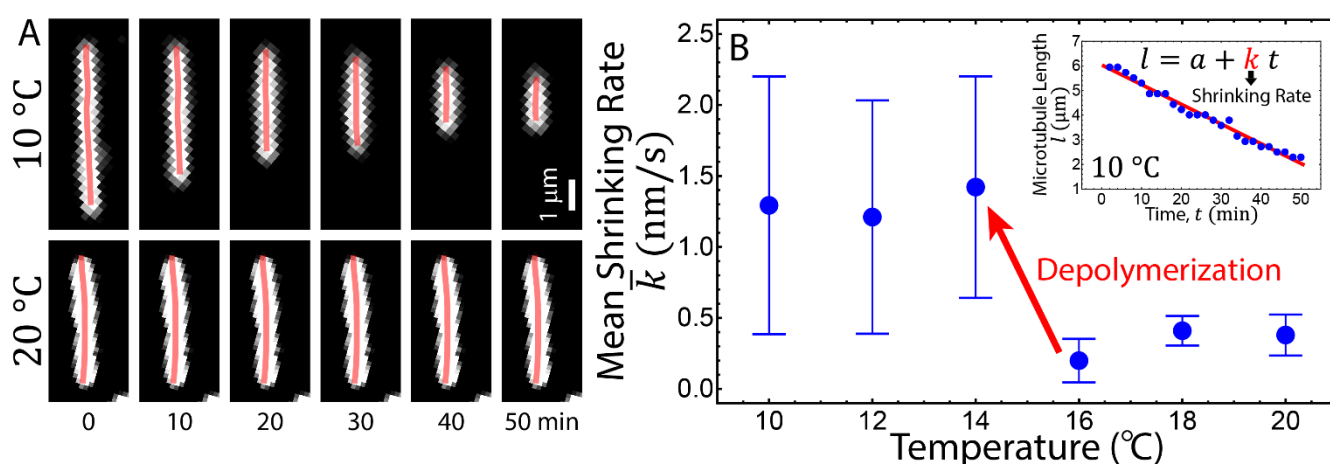


Fig. S2: GMPCPP-Stabilized Microtubules Depolymerize below 16°C. (A) Contrast enhanced images of GMPCPP-stabilized microtubules at 10 and 20°C (top and bottom rows) from $t = 0$ to 50 min (left to right). Each microtubule image was traced by a snake algorithm to measure the microtubule lengths (pink lines)⁵. (B) Mean shrinking rate \bar{k} of microtubule length as a function of temperature. Error bars represent the standard deviations of measurements on 10–13 microtubules. Cooling microtubules below 16°C speeded up shrinking, indicating microtubule depolymerization below 16°C (red arrow). Inset: Time-averaged shrinking rate k was measured by fitting the microtubule length l vs. time t (blue dots) to a line function $l = a + kt$ with a and k as fitting parameters (red line).

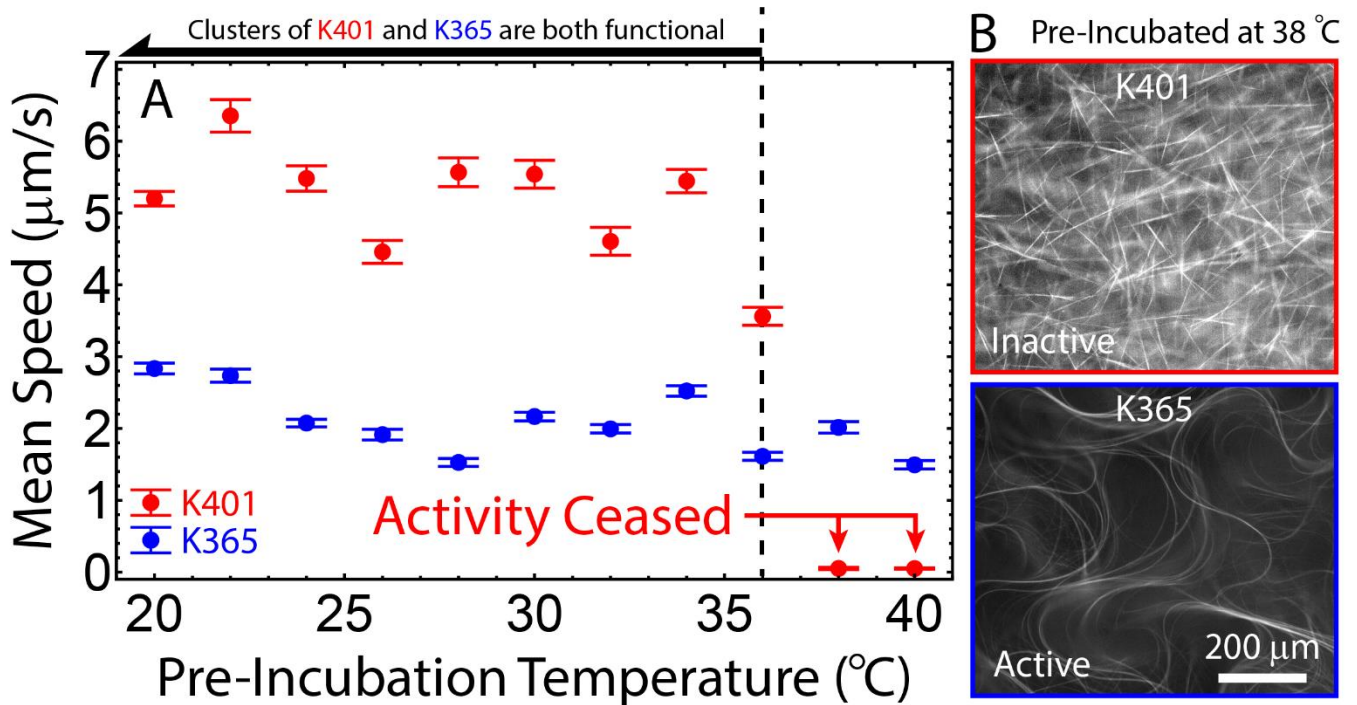


Fig. S3: Temperature-Induced Malfunction for Kinesin Clusters. (A) Mean speed of active fluid flows at 20°C driven by pre-incubated motors as a function of pre-incubation temperature. Error bars represent the standard deviations of time-averaged mean speeds. Pre-incubating K401 clusters at $T \geq 38^{\circ}\text{C}$ ceased flows of active fluids ($\sim 0 \mu\text{m/s}$), in contrast to the case for K365 clusters. Both types of motor clusters were functional below $\sim 36^{\circ}\text{C}$. (B) Images of microtubule-based gels with clusters of K401 (top) and K365 (bottom) pre-incubated at 38°C . The pre-incubated K401 clusters failed to develop long, extensible bundles; the microtubules were stationary. In contrast, the pre-incubated K365 clusters remained capable of sustaining active gel activity.

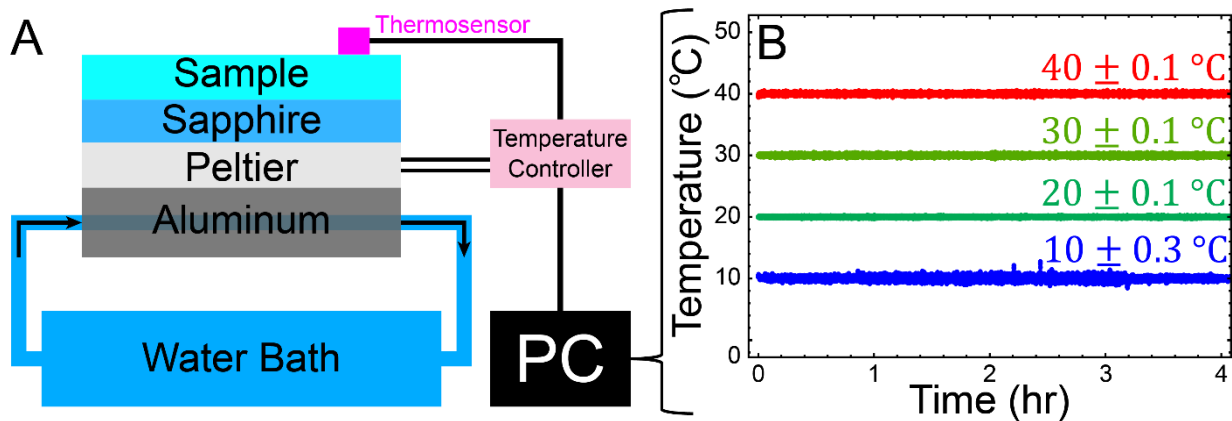


Fig. S4: PID-Based Temperature Control. (A) Schematic of temperature control setup. The setup sat on an aluminum stage whose temperature was regulated by internal circulating flows with a room temperature water bath. The stage supported a peltier, which cooled or heated the sample. To even the sample temperature, a sapphire was inserted between the sample and peltier. The peltier was controlled by a temperature controller that set the power of heating or cooling based on reading the sample temperature with a thermosensor. The read temperatures were recorded on an attached computer to track the temperature stability of each experiment. (B) Recorded sample temperatures for experiments at $10\text{--}40^{\circ}\text{C}$. Sample temperatures were controlled and monitored throughout experiments. Over the course of 4 hours, temperatures fluctuated within $\pm 0.1\text{--}0.3^{\circ}\text{C}$.

Supplementary Movies:

Movie S1: Motion of tracers revealed flows of K401-driven active fluids at 20°C . Time stamp is hour: minute: second.

Movie S2: Microtubules gliding on K401-coated surfaces at 20°C . Time stamp is hour: minute: second.

Movie S3: Increasing temperatures from 20 to 30°C accelerated flows of active fluids, whereas decreasing from 30 to 20°C decelerated flows. Flows of active fluids could be tuned locally with temperature. Time stamp is hour: minute: second.

References

1. T. Sanchez, D. T. N. Chen, S. J. DeCamp, M. Heymann and Z. Dogic, *Nature*, 2012, **491**, 431-434.
2. W. Thielicke and E. J. Stamhuis, *Journal of Open Research Software*, 2014, **2**, e30.
3. C. A. Collins, *The Journal of Cell Biology*, 1987, **105**, 2847-2854.
4. K. J. Böhm, R. Stracke, M. Baum, M. Zieren and E. Unger, *FEBS Letters*, 2000, **466**, 59-62.
5. T. Xu, D. Vavylonis, F.-C. Tsai, G. H. Koenderink, W. Nie, E. Yusuf, I. J. Lee, J.-Q. Wu and X. Huang, *Scientific Reports*, 2015, **5**, 9081.